Carbohydrate Polymers 256 (2021) 117559

Contents lists available at ScienceDirect

Carbohydrate Polymers

journal homepage: www.elsevier.com/locate/carbpol

Fractionation, chemical characterization and immunostimulatory activity of β-glucan and galactoglucan from *Russula vinosa* Lindblad

Hui Zhang [a], Chenchen Li [a], Phoency F.H. Lai [a], Jinshi Chen [b], Fan Xie [a], Yongjun Xia [a], Lianzhong Ai [a,*]

[a] Shanghai Engineering Research Center of Food Microbiology, School of Medical Instruments and Food Engineering, University of Shanghai for Science and Technology, Shanghai, 200093, China

[b] Department of Gynecology, First Affiliated Hospital of Gannan Medical University, Gannan Medical University, Ganzhou, 341000, China

ARTICLE INFO

Keywords:
Russula vinosa Lindblad
Polysaccharides
Fractionation
Chemical structure
Immunostimulatory activity

ABSTRACT

Water-extracted polysaccharides from *Russula vinosa* Lindblad (WRP) were separated into three fractions (WRP-1, WRP-2 and WRP-3) by gradient ethanol precipitation and gel chromatography. Structural characterization indicated that WRP-1 was a branched β-(1→3)-glucan and exhibited rigid helical conformation in aqueous solution with Mw of 2,180 kDa and radius of gyration (Rg) of 123.4 nm. The galactoglucan of WRP-2 and WRP-3 were mainly composed of →6)-Gal*p*-(1→ and →4)-Glc*p*-(1→ terminated by glucose and mannose, presenting much lower Mw (392 and 93.6 kDa) and R*g* (57.6 and 42.6 nm), and more incompact flexible conformation than WRP-1. All fractions showed potential immunostimulatory activity by promoting macrophage proliferation, phagocytosis, as well as the release of nitric oxide and cytokines (TNF-α and IL-1β). WRP-1 with unique structure and conformation showed the best immunostimulatory effects among them. This study suggests that WRP could be explored as natural immunostimulator used in the food and pharmaceutical industry.

1. Introduction

Polysaccharides are considered as one of the main bioactive components from fungi due to their low toxicity, structural diversity and multiple physiological functions (Giavasis, 2014; Nwe, Furuike, & Tamura, 2011; Yu, Shen, Song, & Xie, 2018). They were described as 'Biological Response Modifiers' (BRMs) which could trigger the non-specific reaction of immune system against tumor cells, viral and bacterial infections, inflammations, and provoke an increased synthesis of hormones and cells of the host immune system (Nie, Zhang, Li, & Xie, 2013; Wasser, 2002; Xu, Yan, Tang, Chen, & Zhang, 2014). In addition, some fungal polysaccharides were also reported to possess tumor suppression (Zhang, Cui, Cheung, & Wang, 2007), anti-oxidation (Chen, Xie, Nie, Li, & Wang, 2008), anti-aging (Pan & Lin, 2019), gut-microbiota modulatory (Chang et al., 2015) and hypoglycemic effects (Kim et al., 2001). The fungal β-glucan, such as Lentinan from *Lentinus edodes* and schizophyllan from *Schizophyllum commune*, were even considered to be efficacious in the treatment of gastric, breast, lung, cervical, and colorectal cancers when used in combination with conventional antineoplastic drugs (Giavasis, 2014). Therefore, great interest has been focused on discovering and exploring bioactive polysaccharides from natural fungi to promote human health.

The fungal genus of *Russula* (*R.*) is a highly diverse group of ectomycorrhizal fungi. It is discovered that there are approximate 750 *Russula* species globally, with over 150 species of them distributed in China (Song et al., 2007). To date, several species of *Russula*, such as *R. griseocarnosa* (Liu, Zhang, & Meng, 2018), *R. albonigra* (Krombh.) Fr (Nandi et al., 2012), and *R. virescens* (Sun, Liu, Yang, & Kennedy, 2010; Sun, Zhang, Zhang, & Niu, 2010), have been studied to contain heteropolysaccharides or glucan with different chemical structure as well as anti-tumor, antioxidant and immunostimulant activities. As for the species of *R. vinosa* Lindblad, Liu, Tian, Yan et al. (2014) reported that water-soluble and alkali-soluble polysaccharides from the fruiting bodies could protect the liver from CCl_4-induced hepatic damage *via* antioxidant mechanisms. Our previous study revealed that water-extracted *R. vinosa* Lindblad polysaccharides showed better *in vitro* immunostimulating activity than the alkaline extracts (Li, Lai, Xia, Ai, & Zhang, 2020). However, the structural identity, physicochemical property and immunological activity of *R. vinosa* Lindblad polysaccharides are still lack of knowledge and need to be further elucidated.

* Corresponding author at: University of Shanghai for Science and Technology, 516 Jungong Road, Shanghai, 200093, China.
E-mail addresses: ailianzhong1@126.com, ailianzhong@163.com (L. Ai).

https://doi.org/10.1016/j.carbpol.2020.117559
Received 4 September 2020; Received in revised form 6 December 2020; Accepted 20 December 2020
Available online 28 December 2020

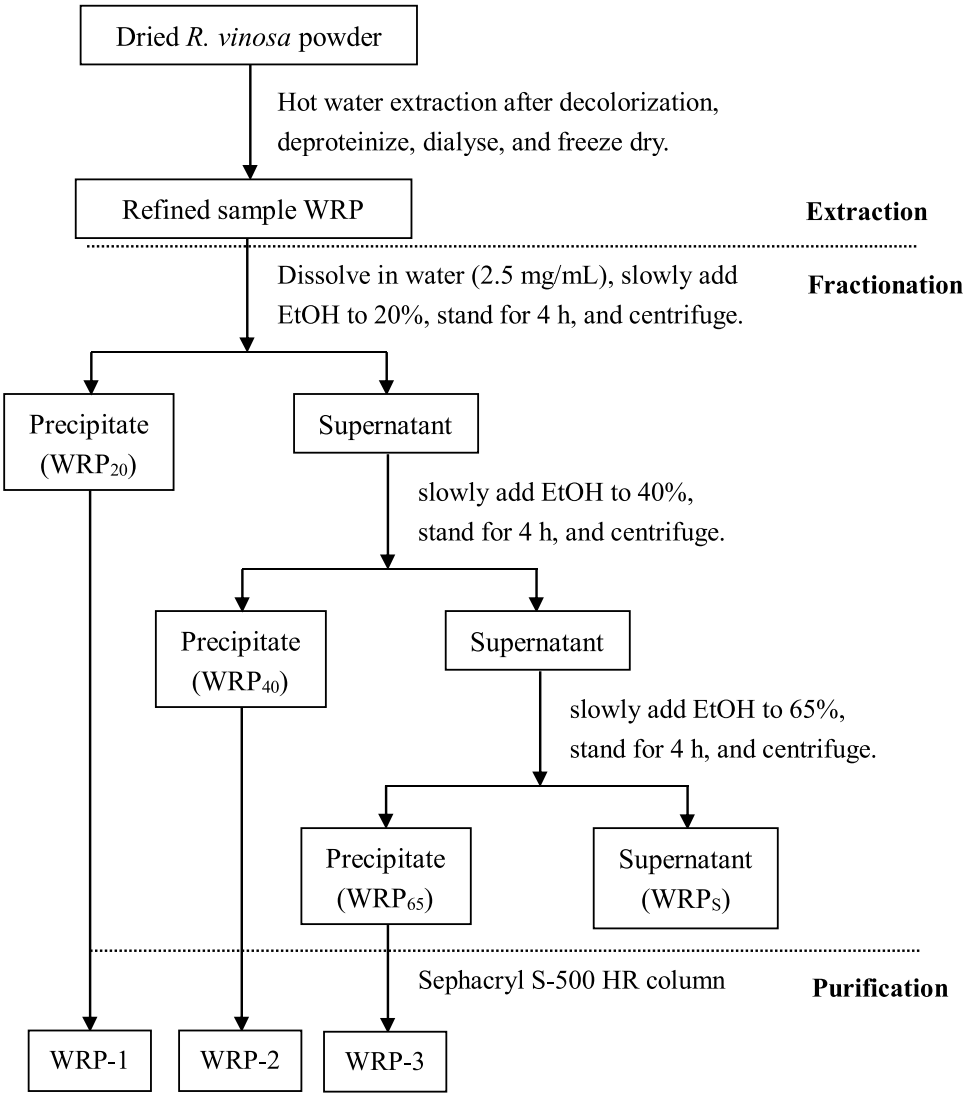

Fig. 1. Extraction and fractionation procedure for polysaccharides from *R. vinosa* Lindblad.

In the present work, the water-extracted polysaccharides from *R. vinosa* Lindblad (WRP) was hypothesized to be fractionated into different fractions with varied structural identity, and thus resulting in the variation of physical and bioactive properties. In light of this, WRP was seperated using gradient ethanol precipitation method, and further purified through gel permeation chromatography on an ÄKTA purifier. The chemical structure and physical properties of different fractions were comparatively characterized by high performance size exclusion chromatography (HPSEC), FT-IR, methylation and GC–MS, and ^{13}C NMR. The immunostimulatory activity was evaluated and compared in terms of cell proliferation, phagocytosis, production of nitric oxide (NO) and cytokines in RAW264.7 cells. The results will provide useful information on the understanding of the structure and bioactivity of *R. vinosa* Lindblad polysaccharides, and will be helpful to promote the economic value of *R. vinosa* Lindblad resources.

2. Material and methods

2.1. Materials and reagents

The dried fruiting bodies of *R. vinosa* Lindblad was sampled from Wuyi Mountain, Fujian Province, China. Mouse macrophage cell line RAW264.7 was purchased from the Cell Resource Center of the Shanghai Institute of Biological Sciences (Shanghai, China). Monosaccharides of D-glucose (Glc), D-xylose (Xyl), D-galactose (Gal), L-rhamnose (Rha), L-fucose (Fuc), D-mannose (Man), D-arabinose (Ara), D-fructose (Fru), D-glucuronic acid (GlcA), and D-galacturonic acid (GalA), lipopolysaccharide (LPS, from *Escherichia coli* 055: B5), deuterium oxide (99.9 % D) and 3-(4,5-dimethyl-2-thiazoly1)-2,5-diphenyl-2-H-tetrazolium bromide (MTT) were purchased from Sigma Chemical Company (St. Louis, MO, USA). Nitric Oxide (NO) assay kit was purchased from Beyotime Biotechnology (Shanghai, China). Mouse TNF-α and IL-1β ELISA kits were purchased from TW-REAGENG (Shanghai, China). All other reagents were of analytical grade from Sinopharm (Shanghai, China) unless specified.

2.2. Extraction and fractionation of polysaccharides from R. vinosa Lindblad

The extraction and fractionation procedure for polysaccharides from *R. vinosa* Lindblad is summarized in Fig. 1. The dried fruiting bodies were firstly crushed and treated with 80 % ethanol solution overnight for degreasing and decolorization. The dried residues were extracted by hot water in a material-to-water ratio of 1: 30 for 3 h at 85 °C. The extracted solution was concentrated and precipitated with three volume of anhydrous ethanol at 4 °C to obtain crude water-extracts. The water-

extracts were re-dissolved in water and deproteinized by Sevage method, successively dialysed (8,000~14,000 Da) against water, concentrated and freeze dried, yielding the refined polysaccharide named WRP.

WRP was firstly fractionated by gradient ethanol precipitation following a previous method (Kang et al., 2011). Briefly, WRP was dissolved in water at the concentration of 2.5 mg/mL, and centrifuged (15,000 ×*g*, 20 min, 25 °C) to obtain homogeneous supernatant. Anhydrous ethanol was added slowly to the supernatant with constant stirring to bring the ethanol concentration to 20 % (v/v), then kept at 4 °C for 4 h to facilitate aggregation. Precipitates were collected by centrifugation (15,000 ×*g*, 20 min, 4 °C) to obtain fraction of WRP_{20}. The concentration of ethanol in the supernatant was stepwise increased to 40 % and 65 % (v/v) to obtain fractions of WRP_{40} and WRP_{65} in a similar manner. Due to the partial co-precipitation of different fractions during gradient precipitation, the three fractions were further purified using a HiPrep 26/60 Sephacryl S-500 HR column (GE Healthcare Life Sciences, USA) on a ÄKTA purifier system (GE Healthcare, Sweden). Samples (5 mL) of different fractions were injected into the column at the concentration of 2 mg/mL. PBS buffer (pH 7.4, 50 mmol/L) was used to elute the samples, and the flow rate was set as 1.3 mL/min. The corresponding purified fractions were designated as WRP-1, WRP-2 and WRP-3, respectively.

2.3. Chemical and monosaccharide composition analysis

Total sugar of refined WRP and different fractions was determined according to the phenol sulfuric acid assay using glucose as the standard (Dubois, Gilles, Hamilton, Rebers, & Smith, 1956). Uronic acid content was measured by the *m*-hydroxybiphenyl method (Blumenkrantz & Asboehansen, 1973) using D-galacturonic acid as the standard. Total protein content was determined with the spectrophotometric assay (Bradford, 1976) using bovine serum albumin as the standard. Total phenolic content (TPC) was expressed as gallic acid equivalent (GAE) per gram of dry weight extract according to Folin–Ciocalteu assay (Slinkard & Singleton, 1977) with some modifications (Zhang et al., 2016).

Monosaccharide composition of samples were conducted by a high performance anion exchange chromatography coupled with pulsed amperometric detection (HPAEC-PAD, Dionex ICS-5000, USA) equipped with a CarboPac™ PA20 column (4 mm × 250 mm, Dionex, USA). Samples (5 mg) were dissolved in 0.5 mL 12 M H_2SO_4 under ice bath for 30 min, then diluted with distilled water to 3 mL and hydrolyzed at 100 ℃ for 2 h. The hydrolysate was diluted 50–100 folds with pure water and injected for analysis directly after filtration with 0.22 μm membrane. The eluents included distilled water (A), 250 mM NaOH solution (B) and 1 M sodium acetate (C). Separation of samples was conducted following a gradient elution procedure (Zhang et al., 2017). Ten monosaccharide standards (Ara, Fru, Fuc, Gal, Glc, Man, Rha, Rib, GalA and GlcA) were used for qualitative and quantitative analysis. All measurements were repeated in triplicate.

2.4. HPSEC assay

The homogeneity and molecular weight of polysaccharides were analyzed by high performance size exclusion chromatography (HPSEC) equipped with a refractive index detector (dRI, Optilab T-rEX, Wyatt Technology, USA), a multi-angle laser light scattering detector (MALLS, DAWN HELEOS-II, Wyatt Technology, USA), a viscosity detector (DP, ViscoStar-II, Wyatt Technology, USA), and a ultraviolet detector (UV, 1260 VWD, Agilent Technologies, USA). An Agilent 1260 Infinity II HPLC system (Agilent Technologies, USA) equipped with a OHpak SB-G 6B guard column and two analytical columns in series, an OHpak SB-803 HQ column and an OHpak SB-805 HQ column (8 mm × 300 mm, Shodex, Tokyo, Japan), was used. The columns, DP and dRI detectors were maintained at 40 °C. The eluent was 0.1 M $NaNO_3$ solution (containing 0.02 wt% NaN_3) at a flow rate of 0.6 mL/min. Samples were prepared at the concentration of 1.0 mg/mL. DN/DC value was adopted as 0.145 mL/g for the calculation. Parameters of weight-average molecular weight (Mw), number-average molecular weight (Mn), radius of gyration (Rg), intrinsic viscosity ([η]) were determined based on Zimm-plots model, from which the conformational properties of the polymers can be extracted (Zhang et al., 2018). ASTRA 7.1.3 software (Wyatt Technology, USA) was used to obtain and analyze the data.

2.5. Fourier transform infrared (FT-IR) spectroscopy analysis

FT-IR spectroscopy of polysaccharide samples was performed by the KBr-disk method within 4000−400 cm^{-1} using an infrared spectrophotometer (Nicolet iS50, Thermo Fisher Scientific, USA). The dried polysaccharide (1 mg) was mixed with KBr powder (200 mg) and pressed into 1 mm pellets for measurement.

2.6. Methylation procedure and GC–MS analysis

The linkage patterns of polysaccharides was studied by methylation and GC–MS analysis according to Ciucanu and Kerek (Ciucanu & Kerek, 1984) and our previous method (Zhang, Zhao et al., 2020). Briefly, 3~5 mg dried samples were dissolved in DMSO with constant stirring overnight. In order to ensure complete dissolution, dried NaOH powder (20 mg) was added to the solution for further 3 h stirring. Methyl iodide (0.3 mL) was dropwise added to the solution in 30 min, following a methylation reaction for 2.5 h at room temperature. Water (0.5 mL) was then added to terminate the reaction. The methylated sample was extracted with 1 mL of CH_2Cl_2, and washed with water for several times. The purified CH_2Cl_2 extract was then passed through a Na_2SO_4 column (0.5 × 15 cm) to remove water. The final CH_2Cl_2 extract was evaporated by a concentrator, hydrolyzed with trifluoroacetic acid (TFA), reduced using sodium borodeuteride, and acetylated with acetic anhydride to derive the partial methylated alditol acetates (PMAAs). The PMAAs were sampled into a GC–MS system (THERMO 1310 GC-ISQ LT MS, USA) equipped with a TG-200MS capillary column (30 m × 0.25 mm, 0.25 mm film thickness, Thermo Fisher, USA) programmed from 160 to 210 °C at 2 °C/min, and then from 210 to 240 °C at 5 °C/min.

2.7. ^{13}C NMR study

Samples (50 mg) were exchanged with deuterium by lyophilizing against deuterium oxide (D_2O) for three times. The deuterated WRP-1 was then dissolved in the solvent of DMSO-d_6/D_2O (6: 1, v/v) at room temperature, while deuterated WRP-2 and WRP-3 were dissolved in D_2O before NMR analysis. The 1D ^{13}C NMR spectra of different fractions were recorded at 151.01 MHz on a Bruker AVIII 600 NMR spectrometer (Brucker, Rheinstetten, Germany) at 298 K.

2.8. Congo red test

Congo red test was used to speculate the helix conformation of WRP modified from previous study (Zhao et al., 2014). The 50 μL of polysaccharide solution (1 mg/mL) was mixed with equal volume of Congo red solution (80 μmol/L) in a 96 well microporous plate. Then, 1 mol/L NaOH solution was slowly added to the mixture until the final concentration of NaOH reached 0−0.5 mol/L. After mixing, the solution was kept at room temperature for 1 h. Congo red solution without polysaccharides was used as control group. The maximum absorption wavelength was determined by scanning in a range from 400 to 600 nm with a microplate reader (SpectraMax i3x instrument, Molecular Devices, USA).

2.9. Assays of immunomodulatory activity in vitro

2.9.1. Cell culture and groups

Murine macrophage cell line RAW264.7 was cultured in DMEM medium containing 10 % fetal bovine serum (FBS), streptomycin (100 μg/mL) and penicillin (100 U/mL) under a humidified atmosphere (5% CO_2, 37 °C). The cells were sub-cultured every 36–48 h to keep the optimum proliferation status for experiments.

The cells (100 μL) were then seeded in tissue culture plate at the concentration of 2×10^5 cells/mL. Subsequently, 100 μL of polysaccharide samples in DMEM medium with different concentrations (25, 50, 100, 200 μg/mL) were added to each well for incubation (24 h). LPS (1 μg/mL) was used as positive control, culture medium in the absence of polysaccharide and LPS was used as the blank control (CON). Each group was conducted in sextuplicate.

2.9.2. Cell viability assay

The effect of samples on the viability of RAW264.7 cells was evaluated by MTT assay (Yu et al., 2013). After incubation the cells (initial concentration of 2×10^5 cells/mL) in 96-well plates for 24 h, 20 μL of MTT solution (5 mg/mL) was added to each well and further incubated for 4 h. After removing the supernatant, 150 μL of DMSO was added to each well, and the mixture was shaken at 30 r/min for 10 min to completely dissolve the crystal formazan. The absorbance was measured at 570 nm by a microplate reader (SpectraMax i3x instrument, Molecular Devices, USA). The cell viability was calculated as the ratio of absorbance of treated cells to untreated cells, expressing as a percentage. The cell morphology of living cells was observed by an inverted fluorescence microscope instrument (Leica DMi8, Leica Microsystems, Germany).

2.9.3. Cell phagocytosis assay

The effect of samples on phagocytic activity of RAW264.7 cells was evaluated by neutral red assay (Nie, Zhu, Ma, Wang, & Hu, 2018). Specifically, the adherent cells were incubated for 24 h with medium alone or polysaccharides or LPS solutions. The supernatants were removed and transferred into a new 96-well plate for nitric oxide assay. Each well with adherent cells was incubated with 100 μL of neutral red solution (dissolving in normal saline, 0.01 % m/v) for 4 h, and then washed twice with PBS. 100 mL of cell lysis buffer (absolute ethanol: acetic acid = 1: 1, v/v) was added to each well at 4 ℃ for 2 h. The absorbance was measured at 540 nm by a multi-functional microplate reader. The absorbance directly reflected the phagocytic activity of macrophages.

2.9.4. Nitric oxide (NO) production

The production of NO by RAW264.7 cells was determined by Griess assay (Yu et al., 2013; Zhang et al., 2016). Briefly, 50 μL Griess reagent I and Griess reagent II were successively mixed into the supernatant of 50 μL cell culture medium at room temperature. After incubation in the dark for 10 min, the absorbance was measured at 570 nm by a multi-functional microplate reader. A standard curve prepared by standards of $NaNO_2$ was used for quantification.

2.9.5. Cytokine secretion

After intervention, the cell culture supernatants were collected to determine the levels of IL-1β and TNF-α by ELISA kits that were specific against murine cytokines. Specifically, 50 μL of the supernatant and 100 μL of horseradish peroxidase-labeled streptavidin (HRP-streptavidin) were added successively to the pre-coated microplate at room temperature and incubated at 37 °C for 60 min. After removing the supernatant, the plate was further washed with buffer for 5 times. Developer substrate (50 μL) was then added to each well and incubated at 37 °C for 15 min in dark. Finally, 50 μL of the stop solution was added and mixed thoroughly. The absorbance was measured at 450 nm. The processing steps of standards were the same as samples.

Table 1
Chemical components and monosaccharide composition of WRP and purified fractions from *R. vinosa* Lindblad.[a]

Sample	WRP	WRP-1	WRP-2	WRP-3
Recovery (%, w/w)	/	36.75 ± 0.86	14.84 ± 0.72	19.82 ± 0.79
Total sugar (%, w/w)	96.73 ± 1.42	97.45 ± 1.12	97.20 ± 1.35	97.81 ± 1.48
Total protein (%, w/w)	1.03 ± 0.11	n.d.[b]	1.16 ± 0.12	n.d.
Total phenolic (%, w/w)	0.67 ± 0.04	n.d.	n.d.	n.d.
Glucose (%)[c]	79.0 ± 1.0	95.6 ± 0.9	64.6 ± 0.9	45.3 ± 1.1
Galactose (%) [c]	19.1 ± 0.5	4.4 ± 0.1	32.9 ± 0.8	50.4 ± 0.7
Mannose (%) [c]	1.9 ± 0.11	n.d.	2.5 ± 0.1	4.3 ± 0.1

[a] All data are shown as mean ± SD with triplicate experiments.
[b] Not detected.
[c] Based on the total sugar content, and shown as the relative molar percentages.

2.10. Statistical analysis

Statistical analysis was performed with SPSS 17.0 software. All experiments were done in triplicate unless specified. All quantitative data were expressed as mean ± SD and differences were considered significant at $p < 0.05$.

3. Results and discussion

3.1. Fractionation and composition analysis

The refined polysaccharide WRP was obtained in a yield of 3.58 % (w/w) from the fruiting bodies of *R. vinosa* Lindblad by hot water extraction and ethanol precipitation. After gradient precipitation at ethanol concentration of 20 %, 40 % and 65 % (v/v), three main precipitates were obtained and designated as WRP_{20}, WRP_{40}, and WRP_{65}, respectively. These ethanol precipitates were further purified using a HiPrep 26/60 Sephacryl S-500 HR column to remove the co-precipitates. Lastly, corresponding fractions of WRP-1, WRP-2 and WRP-3 were obtained with recoveries of 36.75 %, 14.84 % and 19.82 % (w/w), respectively (Fig. 1).

The total sugar, protein, and phenolic contents in WRP and different purified fractions are shown in Table 1. No uronic acid was detected in WRP by the colorimetric method, indicating that WRP was neutral polysaccharide. Small amount of protein and trace phenolic compounds were found in WRP. The high content of total sugar indicated that WRP (96.73 %) and different fractions (97.45 %, 97.20 % and 97.81 % for WRP-1, WRP-2 and WRP-3, respectively) were of high carbohydrate purity. After fractionation, the protein moieties were enriched in WRP-2, and no phenolic impurities was detected in all fractions.

Monosaccharide composition analysis revealed that WRP consisted of glucose (79.0 %), galactose (19.1 %) and mannose (1.9 %). After fractionation, the amount of glucose decreased significantly along the series of WRP-1, WRP-2 and WRP-3 (95.6 %, 64.6 % and 45.3 %, respectively). In contrast, the amount of galactose increased along the same series (4.4 %, 32.9 % and 50.4 %, respectively). Mannose was only found in the fractions of WRP-2 (2.5 %) and WRP-3 (4.3 %). These results demonstrated that WRP-1 might be a glucan with a small amount of galactose, while WRP-2 and WRP-3 were heteropolysaccharides. The composition of WRP-1 fraction was found similar to the results of a previous study, which showed that the water-soluble polysaccharide from *R. vinosa* Lindblad was composed of glucose and galactose in a molar ratio of 41.69: 2.51 (Liu, Tian, Yan et al., 2014), but the fractions of WRP-2 and WRP-3 have not been isolated from *R. vinosa* Lindblad.

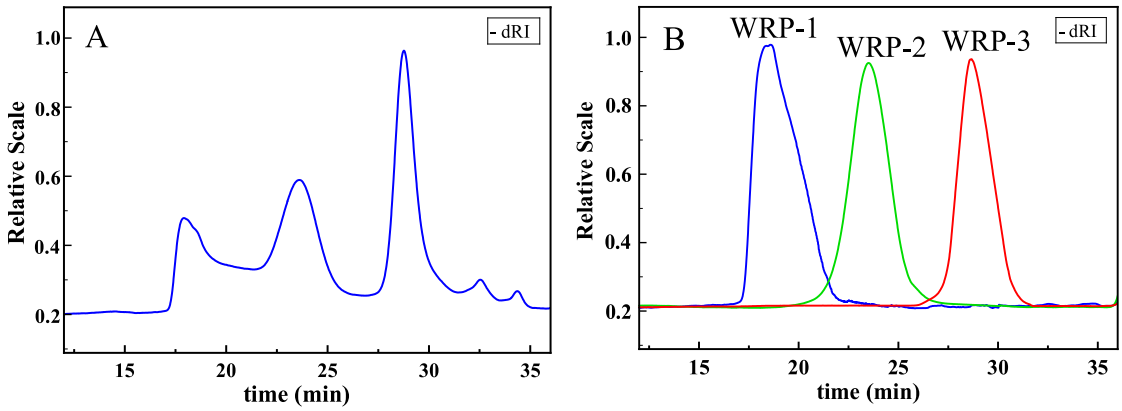

Fig. 2. HPSEC profiles (signals from refractive index (dRI) detector) of refined polysaccharide WRP (A) and purified fractions of WRP-1, WRP-2 and WRP-3 (B) from *R. vinosa* Lindblad.

Table 2
Molecular parameters of different polysaccharide fractions from *R. vinosa* Lindblad.

Parameter	Mw (kDa)	Mn (kDa)	Mw/Mn	[η] (dL/g)	Rg (nm)	[M-H]-α [a]
WRP-1	2,180	2,080	1.05	18.16	123.4	0.90
WRP-2	392	346	1.13	0.24	57.6	0.21
WRP-3	93.6	61.0	1.53	0.13	42.6	0.32

[a] The α value is derived from Mark-Houwink equation ($[\eta] = k\mathrm{Mw}^{\alpha}$).

3.2. HPSEC analysis

The HPSEC profiles of refined sample WRP and different purified fractions as shown in Fig. 2 were used to evaluate the effect of fractionation and homogeneity of purified fractions. The dRI profile of WRP exhibits three major peaks (Fig. 2A), indicating that WRP might possess at least three polymer fractions. After further purification, WRP-1, WRP-2 and WRP-3 all exhibit single peak with different elution time. The polydispersity (Mw/Mn) were calculated as 1.05, 1.13 and 1.53 for WRP-1, WRP-2 and WRP-3, respectively, indicating that these fractions were separated effectively and homogeneous enough for further analysis (Fig. 2B).

Molecular parameters of WRP-1, WRP-2 and WRP-3, including the information of molecular weight, [η], and Rg, were further derived from the HPSEC coupled with multiple detectors and are shown in Table 2. The Mw and Mn of WRP-1 were determined as 2,180 and 2,080 kDa, respectively, with Rg of 123.4 nm and [η] of 18.16 dL/g. The molecular weight of WRP-1 was much higher than the previous reported data from the study of Liu, Tian, Yan et al. (2014). Among the three fractions, the Mw, Mn, Rg and [η] decreased significantly along the series of WRP-1, WRP-2 and WRP-3. The significant difference on the molecular size of different fractions made the gradient ethanol precipitation method feasible for separation.

The α value derived from Mark-Houwink equation ($[\eta] = k\mathrm{Mw}^{\alpha}$) is related to the three-dimensional conformation of polymer chains in the solvent environment. When $\alpha < 0.5$, polymers present a sphere conformation or highly flexibility in an ideal solvent; when $0.5 < \alpha < 0.8$, polymers show a random coil chain; and when $0.8 < \alpha < 2.0$, polymers exhibit a rigid or rod-like conformation (Zhang, Li et al., 2020). The α value of WRP-1 was 0.90 (Table 2), indicating that WRP-1 displayed rigid rod-like structure in 0.1 M $NaNO_3$ solution. However, the solution conformation of WRP-2 and WRP-3 was much more incompact and flexible, as indicated by the low α values. The different solution conformation of WRP-1, WRP-2 and WRP-3 might be related with their different chemical structure, which are elucidated as follows.

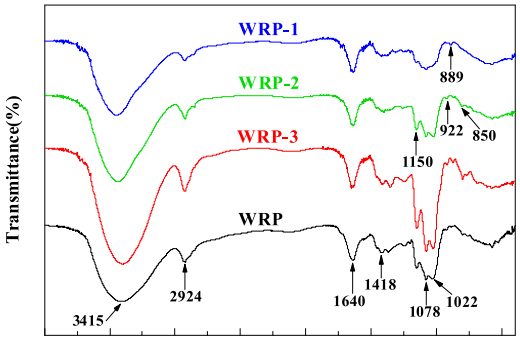

Fig. 3. FT-IR spectrum of different polysaccharide fractions from *R. vinosa* Lindblad.

3.3. FT-IR spectroscopy

The FT-IR spectra of WRP and three purified fractions were recorded at the absorbance mode from 4000 to 400 cm^{-1} at a resolution of 4 cm^{-1} with 128 co-added scans, and the results are shown in Fig. 3. The absorption ranging from 1000 to 4000 cm^{-1} showed the typical carbohydrate features. The broad bands at 3415 cm^{-1} were attributed to the O—H stretching vibration of hydrogen bonds. The bands around 2924 cm^{-1} (3000–2800 cm^{-1}) were caused by the stretching vibration of C—H in a sugar ring. The absorption peaks observed at 1418 cm^{-1} represented the CH_2 bending. The bands at 1150 cm^{-1} were typical for C—O—C stretching vibration of glycosidic linkages. The absorption peaks at 1078 cm^{-1} and 1022 cm^{-1} corresponded to the stretching vibration of C—O—H in pyranose ring structures (Kacurakova, Capek, Sasinkova, Wellner, & Ebringerova, 2000; Mathlouthi & Koenig, 1987).

The area among 800–1200 cm^{-1} "finger print" area for carbohydrates is a good indication of differences in structure among different polysaccharides. Very significant differences were found between WRP-1 and the other fractions. A characteristic absorption at 889 cm^{-1} was observed in WRP-1, indicating the existence of β-type glycosidic linkage. The absorptions at 850 cm^{-1} for the α-configuration were found in WRP-2 and WRP-3 (Chen et al., 2008). These results demonstrated that WRP-1 was mainly in β-configuration, while WRP-2 and WRP-3 were in α-configuration. The absorption at 922 cm^{-1} expressed the D-glucopyranosyl in all fractions (Barker, Bourne, Stacey, & Whiffen, 1954).

3.4. Linkage patterns analysis by methylation and GC–MS

The linkage patterns and content of sugar residues in different polysaccharide fractions of WRP were studied through methylation and GC–MS analysis. The total ions chromatographs (TIC) of PMAAs and

Table 3
Linkage patterns and corresponding percentage content of sugar residues in different polysaccharide fractions from *R. vinosa* Lindblad.

PMAAs	Linkage pattern	Relative percentage (%) [a]		
		WRP-1	WRP-2	WRP-3
2,3,4,6-Me$_4$-Glc*p*	T-Glc*p*-(1→	25.04	18.13	11.99
2,3,4,6-Me$_4$-Man*p*	T-Man*p*-(1→	- [b]	–	6.15
2,4,6-Me$_3$-Glc*p*	→3)-Glc*p*-(1→	35.88	14.12	1.88
2,3,6-Me$_3$-Glc*p*	→4)-Glc*p*-(1→	1.84	20.67	21.12
2,3,4-Me$_3$-Glc*p*	→6)-Glc*p*-(1→	5.44	–	–
2,3,4-Me$_3$-Gal*p*	→6)-Gal*p*-(1→	–	30.11	47.09
4,6-Me$_2$-Glc*p*	→2,3)-Glc*p*-(1→	4.52	–	–
2,4-Me$_2$-Glc*p*	→3,6)-Glc*p*-(1→	25.66	6.84	–
2,3-Me$_2$-Glc*p*	→4,6)-Glc*p*-(1→	–	6.72	5.22
3,4-Me$_2$-Gal*p*	→2,6)-Gal*p*-(1→	–	3.41	6.56
4-Me-Glc*p*	→2,3,6)-Glc*p*-(1→	1.63	–	–

[a] The percentages of each sugar residue were calculated according to the peak areas from the total ion chromatograph of detected PMAAs.
[b] Not found or very low content (< 1%).

corresponding MS spectra of different polysaccharide fractions are provided in Supplementary data (S1, S2 and S3), and the analysis results are listed in Table 3. According to the monosaccharide composition, WRP-1 was considered as a glucan with a small amount of galactose. The GC–MS results indicated that WRP-1 was mainly composed of linear residues of →3)-Glc*p*-(1→ (35.88 %), branched residues of →3,6)-Glc*p*-(1→ (25.66 %), and terminal residues of T-Glc*p*-(1→ (25.04 %), with small amounts of →6)-Glc*p*-(1→ (5.44 %), →2,3)-Glc*p*-(1→ (4.52 %), →4)-Glc*p*-(1→ (1.84 %), and tri-substituted residues of →2,3,6)-Glc*p*-(1→ (1.63 %). No galactose residues were found from GC–MS results after methylation. By combining the FT-IR analysis and previous studies (Liu, Zhang, Tang et al., 2014; Nandi et al., 2014), WRP-1 was speculated to be a β-(1→3)-glucan with branches at *O*-6 position, occasionally at *O*-2 position of glucose.

As to the fractions of WRP-2 and WRP-3, the main sugar residues of →6)-Gal*p*-(1→ increased from 30.11%–47.09%, while residues of →3)-Glc*p*-(1→ decreased from 14.12 % to 1.88 %, with comparative content of →4)-Glc*p*-(1→ (20.67 % and 21.12 %, respectively). The terminal residues were of T-Glc*p*-(1→ (18.13 % and 11.99 %, respectively), and T-Man*p*-(1→ (6.15 %) was also found in WRP-3. The branched residues in WRP-2 were deduced as →3,6)-Glc*p*-(1→ (6.84 %), →4,6)-Glc*p*-(1→ (6.72 %), and →2,6)-Gal*p*-(1→ (3.41 %), while lower content of →4,6)-Glc*p*-(1→ (5.22 %), and higher content of →2,6)-Gal*p*-(1→ (6.56 %) were detected in WRP-3. These results suggested that fractions of WRP-2 and WRP-3 might be the same type of galactoglucan composing of glucose, galactose and minor content of mannose. This kind of galactoglucan was also found in other fungi, but with different ratio and linkages of sugar residues (Manna et al., 2017; Wold et al., 2018). The degrees of branching (DB) of different fractions were calculated using the following equation according to Hawker, Lee, and Fréchet (1991):

$$\mathrm{DB} = \frac{\text{number of dentric units} + \text{number of terminal units}}{\text{total number of units}} \times 100\% \quad (1)$$

The results showed the DB of WRP-1, WRP-2 and WRP-3 as 58.48 %, 35.10 % and 29.92 %, respectively, indicating that the DB decreased during the fractionation process.

3.5. ^{13}C NMR analysis

The ^{13}C NMR (Fig. 4) was conducted to study the structural features of different polysaccharide fractions. As shown in Fig. 4A, the anomeric carbon signals of different sugar residues in WRP-1 were found around at δ 103.22 ppm, and the full ^{13}C NMR spectrum was similar to the reported spectrum of β-(1→3, 1→6)-glucan (Liu, Zhang, Tang et al., 2014). The low signal at δ 98.96 ppm was ascribed to the small impurity of other fractions (WRP-2 and WRP-3) which were difficult to be removed. Combining the results of monosaccharide composition, FT-IR spectrum, methylation and GC–MS, WRP-1 was proved to be a branched β-(1→3)-glucan. The ^{13}C NMR spectra of WRF-2 and WRF-3 (Fig. 4B and C) showed that chemical shifts of anomeric carbons were in the range of δ 97.85–99.92 ppm. This indicated that the sugar residues in WRF-2 and WRF-3 were mainly in α-configuration (Cui, 2005), which was consistent with results of FT-IR spectra.

To sum up, the structural features showed significant differences among the fractions of WRP-1, WRP-2 and WRP-3. WRP-1 was identified to be a branched β-(1→3)-glucan with high molecular weight, while WRP-2 and WRP-3 were proposed to be α-galacoglucans which were composed of glucose, galactose and minor content of mannose. Similar types of polysaccharides have been found to exist in other mushrooms, such as *Lentinus edodes* (Xu et al., 2014) and *Ganoderma* (Nie et al., 2013), and other species of *Russula*, such as *R. albonigra* (Krombh.) Fr (Nandi et al., 2012). These polysaccharides were considered to possess high bioactivities on immunomodulatory, antioxidant and anti-tumor. This implies that the polysaccharides from *R. vinosa* Lindblad might be a good bioactive resource to promote human health.

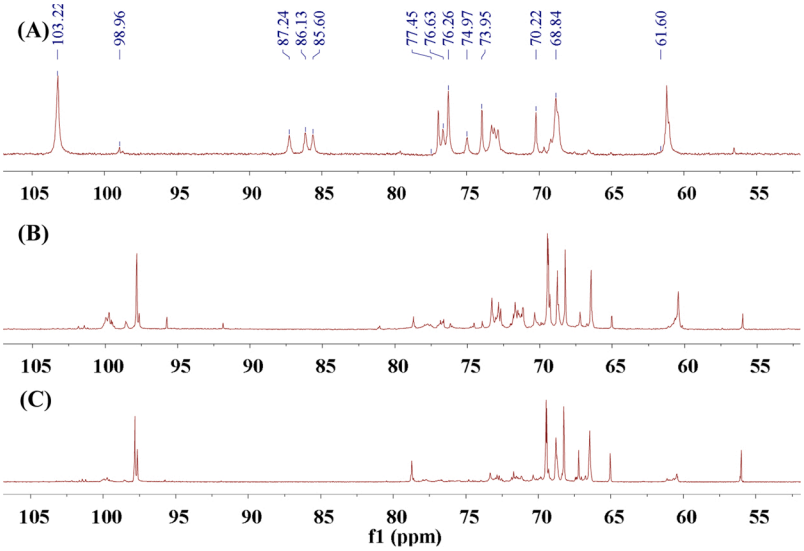

Fig. 4. ^{13}C NMR spectra of polysaccharide fractions of WRP-1 (A), WRP-2 (B) and WRP-3 (C) from *R. vinosa* Lindblad recorded at 298 K. The WRP-1 was dissolved in the solvent of DMSO-d_6/D_2O (6: 1, v/v), while WRP-2 and WRP-3 were dissolved in D_2O solvent.

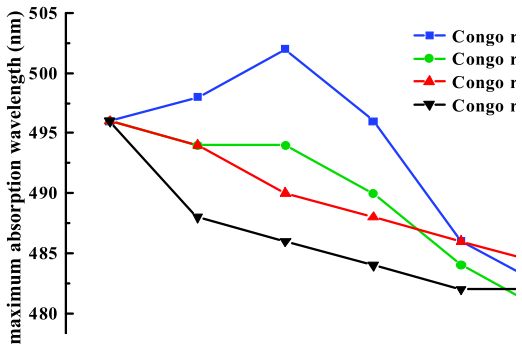

Fig. 5. Changes of maximum absorption wavelength of mixture of Congo red-polysaccharide fractions from *R. vinosa* Lindblad at various concentrations of NaOH.

3.6. Helix-coil transition analysis

The presence of polysaccharides in a helical conformation would form complexes with Congo red in dilute NaOH solutions and induce a red shift of the visible maximum absorption in comparison with pure Congo red. This phenomenon provides a rapid method to detect the helical-coil transition property of polysaccharides (Wang et al., 2014; Zhao et al., 2014). The maximum absorption wavelength (λ_{max}) of Congo red with different polysaccharide fractions at various NaOH concentrations are shown in Fig. 5. Compared with Congo red solution, the Congo red-WRP-1 complex showed a distinct red shift of λ_{max} from 496 nm to 503 nm along with the increase of NaOH concentration to 0.2 M, then blue shift appeared slowly as NaOH concentration increased from 0.3 to 0.5 M. In contrast, the blue shifts of Congo red-WRP-2 and Congo red-WRP-3 complexes were found, and Congo red-WRP-3 complex showed similar trend with the pure Congo red solution. These results revealed that WRP-1 possessed an ordered helical structure (Ogawa & Hatano, 1978), while WRP-2 and WRP-3 presented loose conformation in aqueous solution, which were consistent with the HPSEC results. With the increase of NaOH concentration (0.3−0.5 M), the ordered helical structure of WRP-1 was broken down, presenting a helix-coil transition under the high concentration treatment of alkaline solution. The conformational transition property of WRP-1 was similar to lentinan extracted from *Lentinus edodes* (Wang et al., 2014). The helical structure might be attributed to the β-(1→3)-glucan backbone with short branches which could facilitate the formation of helical structure *via* intermolecular hydrogen bond, while strong alkaline condition destroyed the intermolecular interaction, resulting in helical-coil transition. The λ_{max} value of the complex resulting from Congo red-WRP-2 was higher than that of Congo red-WRP-3 when the concentration of NaOH was at 0.2−0.3 M, indicating a stronger inter-chain hydrogen bond being connected in WRP-2.

3.7. Evaluation of immunomodulatory activity on macrophages

3.7.1. Effects on proliferation and morphology of RAW264.7 cells

Macrophages exist in virtually all tissues and have long been considered as an important cell of host defense against microbial invaders and malignancies (Dunn, Barke, Ewald, & Simmons, 1987). In

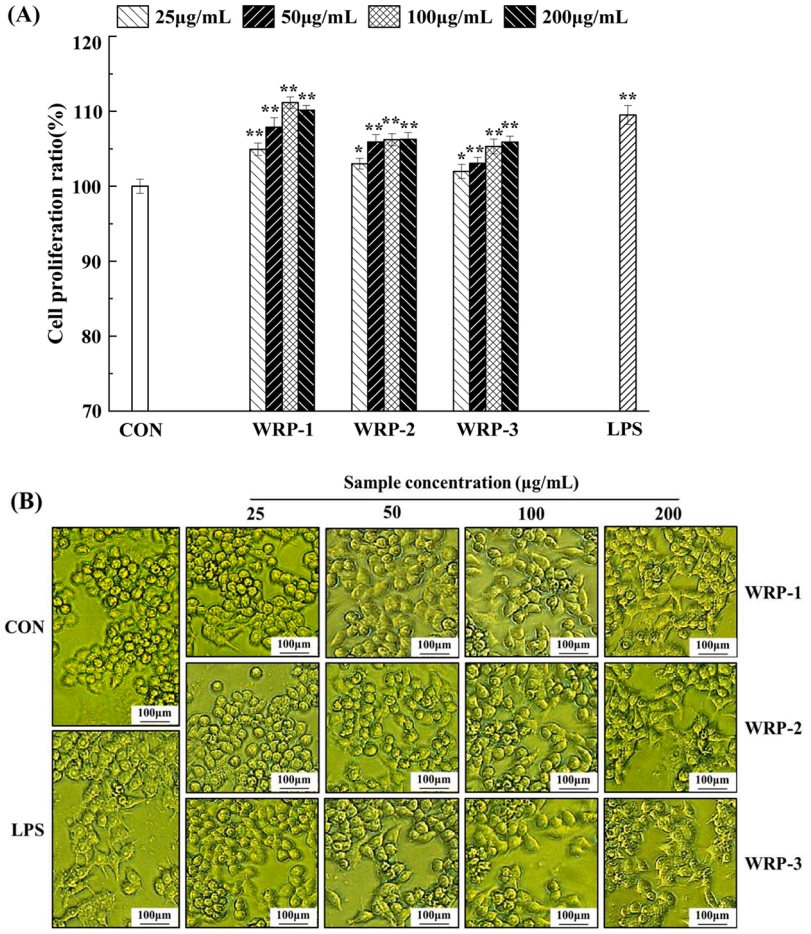

Fig. 6. Effects of different polysaccharide fractions from *R. vinosa* Lindblad on the proliferation rate (A) and morphology (B) of RAW264.7 cells. Cells were cultured with different concentrations (25, 50, 100, 200 μg/mL) of polysaccharide fractions for 24 h. LPS (1 μg/mL) was used as positive control. $^{*}p < 0.05$, $^{**}p < 0.01$ compared with the CON group, n = 6. The bar in (B) represents 100 μm.

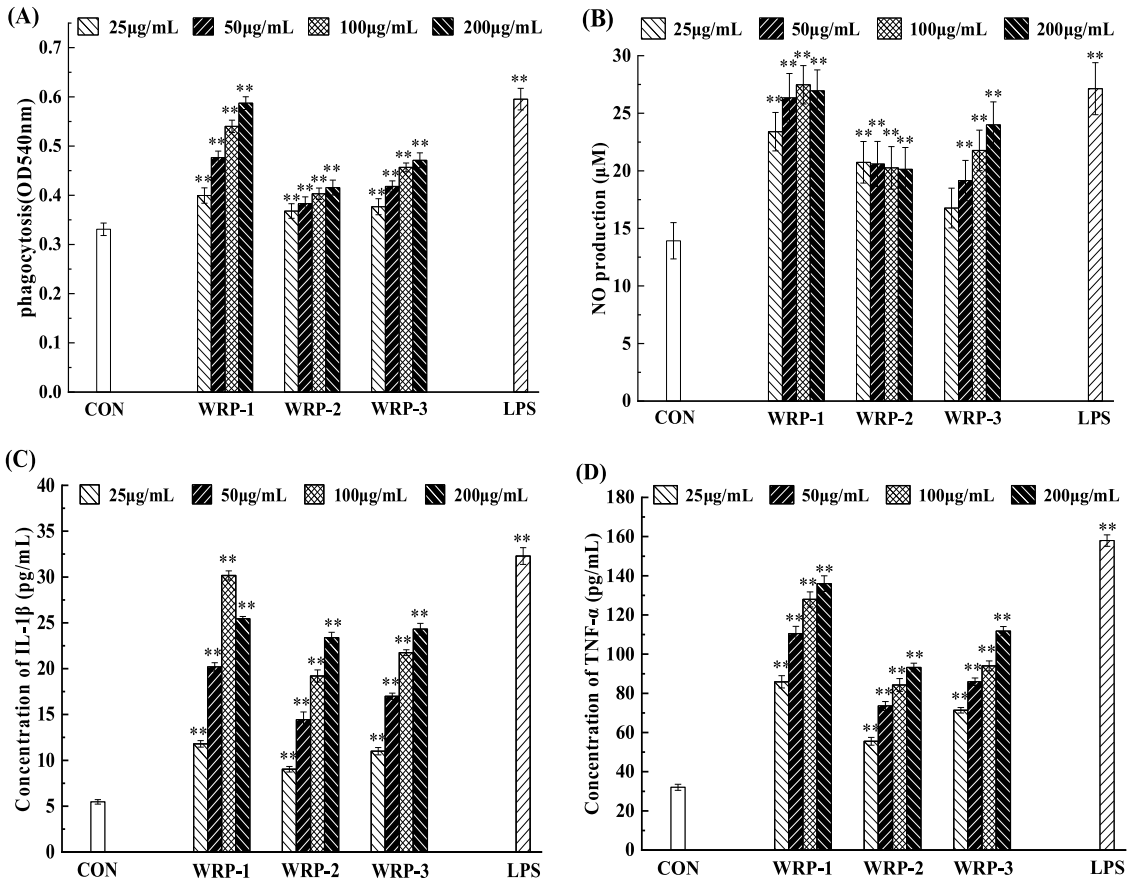

Fig. 7. Effects of different polysaccharide fractions from *R. vinosa* Lindblad on the phagocytic ability (A), NO production (B), cytokine of IL-1β secretion (C), and cytokine of TNF-α secretion (D) of RAW264.7 cells. Cells were cultured with different concentrations (25, 50, 100, 200 μg/mL) of polysaccharides for 24 h. LPS (1 μg/mL) was the positive control. $^{*}p < 0.05$, $^{**}p < 0.01$ compared with the CON group, n = 6.

addition, macrophages can respond not only to endogenous stimuli generated by injury or infection, but also to signals produced by antigen-specific immune cells (Mosser & Edwards, 2008). The effects of three purified polysaccharide fractions on macrophage viability were assayed by MTT method. The proliferation of RAW264.7 cells with the treatment of various concentrations (25, 50, 100, and 200 μg/mL) of WRP-1, WRP-2 and WRP-3 are shown in Fig. 6A. Compared with the blank control (CON), all samples exhibited a significant stimulatory effect on RAW264.7 cells proliferation ($p < 0.05$). The cell viability of WRP-1 on macrophage was the highest among the three fractions at the same concentration.

Furthermore, the morphological features of RAW264.7 cells after treatment with polysaccharides were observed by microscopy. Normally, macrophages are circular or ovoid in shape (as shown in the CON group of Fig. 6B). After encountering stimuli, the surface edges of macrophages would form filopodia and lamellipodia, leading to morphological changes (Liu et al., 2017). In comparison to the CON group, the morphological features of RAW264.7 cells demonstrated obvious changes after treatment with different polysaccharide fractions (Fig. 6B). With growing concentrations of WRP-1, WRP-2 and WRP-3, spindle-shaped or irregular cells increased and a large number of pseudopods appeared. These results showed the characteristics of macrophage activation after treatment with different polysaccharide fractions from *R. vinosa* Lindblad.

3.7.2. Effects on phagocytosis of RAW264.7 cells

Phagocytosis is an important index to evaluate the immune response of macrophages. After phagocytic uptake of invader, macrophages turn their role into antigen-presenting cells with expression of higher levels of costimulatory molecules, and then mediate an interaction between T cells and macrophages (Fidler & Kleinerman, 1993). The effects of different polysaccharide fractions on the phagocytic ability of RAW264.7 cells were evaluated by neutral red assay. As shown in Fig. 7A, all polysaccharide fractions significantly enhanced the uptake of neutral red ($p < 0.01$), presenting dose-dependency in comparison to the CON group. Among the three fractions, WRP-1 showed the best phagocytic enhancement effect, followed by WRP-3 and then WRP-2. As phagocytes acted as regulatory and effector cells in the immune system, the enhancement of the phagocytic function by polysaccharide fractions from *R. vinosa* Lindblad meant elevation of the innate immune response.

3.7.3. Effects on NO production of RAW264.7 cells

NO is an important mediator in the process of immune regulation, involving in the regulation of apoptosis and in host defenses against microorganisms and tumor cells (Schepetkin & Quinn, 2006). Macrophages could produce a large amount of NO to exert non-specific immunity. Fig. 7B shows the effects of different polysaccharide fractions on NO production of RAW264.7 cells. All samples of WRP-1, WRP-2 and WRP-3 significantly increased NO production of macrophages, compared with the CON group ($p < 0.01$). WRP-1 showed the highest NO level among the three fractions. With the increase of sample concentration, the NO production of WRP-1 group climbed gradually to the concentration of 200 μg/mL, while the NO level of WRP-3 group grew in a dose-dependent manner. In contrast, the concentration increase of WRP-2 had no significant effect on the NO production, or contrarily reduced the NO level slowly. In conclusion, polysaccharides from *R. vinosa* Lindblad could promote the production of NO after activating the macrophages, and WRP-1 exhibited the best ability to adjust the

production of NO.

3.7.4. Effects on IL-1β and TNF-α release of RAW264.7 cells

Cytokines are intercellular signaling proteins or peptides involved in modulating immune response and inflammatory reactions, particularly during infection and trauma. In addition, cytokines can affect cell differentiation, proliferation and apoptosis (Haddad, 2002; Wang, Yang, Zhao, Lu, & Zhu, 2017). IL-1β and TNF-α are two typical pro-inflammatory cytokines, which can be secreted by activated macrophages with immunomodulatory properties. In the current study, the effects of different polysaccharide fractions on the production of IL-1β and TNF-α by RAW264.7 cells were determined by ELISA. Compared with the CON group, WRP-1, WRP-2 and WRP-3 significantly promoted the release of IL-1β (Fig. 7C) and TNF-α (Fig. 7D) in a dose-dependent manner, except that IL-1β was promoted by WRP-1 at the concentration of 200 μg/mL. At the same concentration, WRP-1 showed much better effect on the release of IL-1β and TNF-α than WRP-2 and WRP-3, but no significant difference was found between WRP-2 and WRP-3 groups. When the concentration of WRP-1 increased to 100 μg/mL, the amount of released IL-1β reached up to 30.12 pg/mL, slightly lower than that stimulated by LPS (32.29 pg/mL). These results indicated that all polysaccharide fractions from *R. vinosa* Lindblad could exert immune effects by stimulating RAW264.7 cells to secrete cytokines of IL-1β and TNF-α, and WRP-1 exhibited the highest levels, which comply with the results as aforementioned.

4. Conclusions

In this study, three purified polysaccharides of WRP-1, WRP-2 and WRP-3 with Mw of 2,180, 392 and 93.6 kDa, respectively, were successfully extracted and fractionated from the fruiting bodies of *R. vinosa* Lindblad by gradient ethanol precipitation and gel permeation chromatography techniques. WRP-1, which had the highest molecular weight, was proposed to be a branched β-(1→3)-glucan and showed ordered helical conformation in aqueous solution. However, WRP-2 and WRP-3 consisting of glucose, galactose and mannose in different ratios presented high flexiblility, which might be due to the high content of (1→6)-linkages in the molecular chain. *In vitro* cellular experiments showed that all fractions of WRP-1, WRP-2 and WRP-3 exhibited immunostimulatory activity without cytotoxicity. WRP-1 more effectively promoted the mouse macrophages proliferation, phagocytosis, NO production and cytokines release than WRP-2 and WRP-3. It is reported that molecular weight and a helical conformation are known to be important factors for the immune-stimulating activity of β-(1→3)-glucan (Bohn & BeMiller, 1995; Zhang, Li, Wang, Zhang, & Cheung, 2011). Therefore, it is speculated that the helical structure and high molecular weight would be one of the key features for WRP-1 to exhibit immunostimulatory activity. However, further work needs to be done to confirm the proposal by elucidating the fine structures and structure-bioactivity relationship of WRP.

CRediT authorship contribution statement

Hui Zhang: Conceptualization, Methodology, Project administration, Writing - original draft. **Chenchen Li:** Project administration, Formal analysis. **Phoency F.H. Lai:** Methodology, Writing - review & editing. **Jinshi Chen:** Methodology, Project administration. **Fan Xie:** Methodology, Writing - review & editing. **Yongjun Xia:** Validation. **Lianzhong Ai:** Supervision.

Acknowledgements

The financial support for this study by the Shanghai Agriculture Applied Technology Development Program, China (No. 2019-02-08-00-07-F01152), the National Science Fund for Distinguished Young Scholars (No. 32025029), and Shanghai Engineering Research Center of Food Microbiology (No. 19DZ2281100), is gratefully acknowledged.

Appendix A. Supplementary data

Supplementary material related to this article can be found, in the online version, at doi:https://doi.org/10.1016/j.carbpol.2020.117559.

References

Barker, S. A., Bourne, E. J., Stacey, M., & Whiffen, D. H. (1954). Infra-red spectra of carbohydrates. Part I. Some derivatives of D-glucopyranose. *Journal of The Chemical Society (resumed)*, 171–176.

Blumenkrantz, N., & Asboehansen, G. (1973). New method for quantitative determination of uronic acids. *Analytical Biochemistry, 54*(2), 484–489.

Bohn, J. A., & BeMiller, J. N. (1995). (1→3)-β-d-glucans as biological response modifiers: A review of structure-functional activity relationships. *Carbohydrate Polymers, 28*(1), 3–14.

Bradford, M. M. (1976). A rapid and sensitive method for the quantitation of microgram quantities of protein utilizing the principle of protein-dye binding. *Analytical Biochemistry, 72*(1), 248–254.

Chang, C., Lin, C., Lu, C., Martel, J., Ko, Y., Ojcius, D. M., et al. (2015). *Ganoderma lucidum* reduces obesity in mice by modulating the composition of the gut microbiota. *Nature Communications, 6*(1), 7489–7489.

Chen, Y., Xie, M., Nie, S., Li, C., & Wang, Y. (2008). Purification, composition analysis and antioxidant activity of a polysaccharide from the fruiting bodies of *Ganoderma atrum*. *Food Chemistry, 107*(1), 231–241.

Ciucanu, I., & Kerek, F. (1984). A simple and rapid method for the permethylation of carbohydrates. *Carbohydrate Research, 131*(2), 209–217.

Cui, S. W. (2005). Structural analysis of polysaccharides. In S. W. Cui (Ed.), *Food carbohydrates: Chemistry, physical properties, and applications*. Boca Raton, FL: CRC Press.

Dubois, M., Gilles, K. A., Hamilton, J. K., Rebers, P. A., & Smith, F. (1956). Colorimetric method for determination of sugars and related substances. *Analytical Chemistry, 28*(3), 350–356.

Dunn, D. L., Barke, R. A., Ewald, D. C., & Simmons, R. L. (1987). Macrophages and translymphatic absorption represent the first line of host defense of the peritoneal cavity. *Archives of Surgery, 122*(1), 105–110.

Fidler, I. J., & Kleinerman, E. S. (1993). Therapy of cancer metastasis by systemic activation of macrophages: From the bench to the clinic. *Research in Immunology, 144*(4), 284–287.

Giavasis, I. (2014). Bioactive fungal polysaccharides as potential functional ingredients in food and nutraceuticals. *Current Opinion in Biotechnology, 26*, 162–173.

Haddad, J. J. (2002). Cytokines and related receptor-mediated signaling pathways. *Biochemical and Biophysical Research Communications, 297*(4), 700–713.

Hawker, C. J., Lee, R., & Fréchet, J. M. J. (1991). One-step synthesis of hyperbranched dendritic polyesters. *Journal of the American Chemical Society, 113*(12), 4583–4588.

Kacurakova, M., Capek, P., Sasinkova, V., Wellner, N., & Ebringerova, A. (2000). FT-IR study of plant cell wall model compounds: Pectic polysaccharides and hemicelluloses. *Carbohydrate Polymers, 43*(2), 195–203.

Kang, J., Cui, S. W., Chen, J., Phillips, G. O., Wu, Y., & Wang, Q. (2011). New studies on gum ghatti (*Anogeissus latifolia*) part I. Fractionation, chemical and physical characterization of the gum. *Food Hydrocolloids, 25*(8), 1984–1990.

Kim, D., Yang, B., Jeong, S., Park, J., Cho, S., Das, S., et al. (2001). Production of a hypoglycemic, extracellular polysaccharide from the submerged culture of the mushroom, *Phellinus linteus*. *Biotechnology Letters, 23*(7), 513–517.

Li, C., Lai, P. F. H., Xia, Y., Ai, L., & Zhang, H. (2020). Comparison of chemical composition and cellular immune activity of polysaccharide extracts obtained from different parts of *Russula vinosa*. *Food and Fermentation Industries, 46*(9), 115–121.

Liu, F., Zhang, X., Ling, P., Liao, J., Zhao, M., Mei, L., et al. (2017). Immunomodulatory effects of xanthan gum in LPS-stimulated RAW 264.7 macrophages. *Carbohydrate Polymers, 169*, 65–74.

Liu, Y., Zhang, J., & Meng, Z. (2018). Purification, characterization and anti-tumor activities of polysaccharides extracted from wild *Russula griseocarnosa*. *International Journal of Biological Macromolecules, 109*, 1054–1060.

Liu, Q., Tian, G., Yan, H., Geng, X., Cao, Q., Wang, H., et al. (2014). Characterization of polysaccharides with antioxidant and hepatoprotective activities from the wild edible mushroom *Russula vinosa* Lindblad. *Journal of Agricultural and Food Chemistry, 62*(35), 8858–8866.

Liu, Y., Zhang, J., Tang, Q., Yang, Y., Guo, Q., Wang, Q., et al. (2014). Physicochemical characterization of a high molecular weight bioactive β-d-glucan from the fruiting bodies of *Ganoderma lucidum*. *Carbohydrate Polymers, 101*, 968–974.

Manna, D. K., Maity, P., Nandi, A. K., Pattanayak, M., Panda, B. C., Mandal, A. K., et al. (2017). Structural elucidation and immunostimulating property of a novel polysaccharide extracted from an edible mushroom *Lentinus fusipes*. *Carbohydrate Polymers, 157*, 1657–1665.

Mathlouthi, M., & Koenig, J. L. (1987). Vibrational spectra of carbohydrates. *Advances in Carbohydrate Chemistry and Biochemistry, 44*, 7–89.

Mosser, D. M., & Edwards, J. P. (2008). Exploring the full spectrum of macrophage activation. *Nature Reviews Immunology, 8*(12), 958–969.

Nandi, A. K., Samanta, S., Maity, S., Sen, I. K., Khatua, S., Devi, K. S. P., et al. (2014). Antioxidant and immunostimulant β-glucan from edible mushroom *Russula albonigra* (Krombh.) Fr. *Carbohydrate Polymers, 99*, 774–782.

Nandi, A. K., Sen, I. K., Samanta, S., Maity, K., Devi, K. S. P., Mukherjee, S., et al. (2012). Glucan from hot aqueous extract of an ectomycorrhizal edible mushroom, *Russula albonigra* (Krombh.) Fr.: structural characterization and study of immunoenhancing properties. *Carbohydrate Research, 363*, 43–50.

Nie, C., Zhu, P., Ma, S., Wang, M., & Hu, Y. (2018). Purification, characterization and immunomodulatory activity of polysaccharides from stem lettuce. *Carbohydrate Polymers, 188*, 236–242.

Nie, S., Zhang, H., Li, W., & Xie, M. (2013). Current development of polysaccharides from *Ganoderma*: Isolation, structure and bioactivities. *Bioactive Carbohydrates and Dietary Fibre, 1*(1), 10–20.

Nwe, N., Furuike, T., & Tamura, H. (2011). Production, properties and applications of fungal cell wall polysaccharides: Chitosan and glucan. In R. Jayakumar, M. Prabaharan, & R. A. A. Muzzarelli (Eds.), *Chitosan for biomaterials II* (pp. 187–207). Berlin, Heidelberg: Springer Berlin Heidelberg.

Ogawa, K., & Hatano, M. (1978). Circular dichroism of the complex of a (1→3)-β-D-glucan with Congo Red. *Carbohydrate Research, 67*(2), 527–535.

Pan, Y., & Lin, Z. (2019). Anti-aging effect of Ganoderma (Lingzhi) with health and fitness. In Z. Lin, & B. Yang (Eds.), *Ganoderma and health: pharmacology and clinical application* (pp. 299–309). Singapore: Springer Singapore.

Schepetkin, I. A., & Quinn, M. T. (2006). Botanical polysaccharides: Macrophage immunomodulation and therapeutic potential. *International Immunopharmacology, 6*(3), 317–333.

Slinkard, K., & Singleton, V. L. (1977). Total phenol analysis: Automation and comparison with manual methods. *American Journal of Enology and Viticulture, 28*(1), 49–55.

Song, B., Li, T. H., Wu, X. L., Li, J. J., Shen, Y. H., & Lin, Q. Y. (2007). Known species of *Russula* from China and their distribution. *Journal of Fungal Research, 5*(1), 20–42.

Sun, Y. X., Liu, J. C., Yang, X. D., & Kennedy, J. F. (2010). Purification, structural analysis and hydroxyl radical-scavenging capacity of a polysaccharide from the fruiting bodies of *Russula virescens*. *Process Biochemistry, 45*(6), 874–879.

Sun, Z., Zhang, L., Zhang, B., & Niu, T. (2010). Structural characterisation and antioxidant properties of polysaccharides from the fruiting bodies of *Russula virescens*. *Food Chemistry, 118*(3), 675–680.

Wang, K., Wang, J., Li, Q., Zhang, Q., You, R., Cheng, Y., et al. (2014). Structural differences and conformational characterization of five bioactive polysaccharides from *Lentinus edodes*. *Food Research International, 62*, 223–232.

Wang, M., Yang, X., Zhao, J., Lu, C., & Zhu, W. (2017). Structural characterization and macrophage immunomodulatory activity of a novel polysaccharide from Smilax glabra Roxb. *Carbohydrate Polymers, 156*, 390–402.

Wasser, S. P. (2002). Medicinal mushrooms as a source of antitumor and immunomodulating polysaccharides. *Applied Microbiology and Biotechnology, 60*(3), 258–274.

Wold, C. W., Kjeldsen, C., Corthay, A., Rise, F., Christensen, B. E., Duus, J.Ø., et al. (2018). Structural characterization of bioactive heteropolysaccharides from the medicinal fungus *Inonotus obliquus* (Chaga). *Carbohydrate Polymers, 185*, 27–40.

Xu, X., Yan, H., Tang, J., Chen, J., & Zhang, X. (2014). Polysaccharides in *Lentinus edodes*: Isolation, structure, immunomodulating activity and future prospective. *Critical Reviews in Food Science and Nutrition, 54*(4), 474–487.

Yu, Q., Nie, S., Li, W., Zheng, W., Yin, P., Gong, D., et al. (2013). Macrophage immunomodulatory activity of a purified polysaccharide isolated from *Ganoderma atrum*. *Phytotherapy Research, 27*(2), 186–191.

Yu, Y., Shen, M., Song, Q., & Xie, J. (2018). Biological activities and pharmaceutical applications of polysaccharide from natural resources: A review. *Carbohydrate Polymers, 183*, 91–101.

Zhang, H., Cui, S. W., Nie, S., Chen, Y., Wang, Y., & Xie, M. (2016). Identification of pivotal components on the antioxidant activity of polysaccharide extract from *Ganoderma atrum*. *Bioactive Carbohydrates and Dietary Fibre, 7*(2), 9–18.

Zhang, H., Nie, S., Cui, S. W., Xu, M., Ding, H., & Xie, M. (2017). Characterization of a bioactive polysaccharide from *Ganoderma atrum*: Re-elucidation of the fine structure. *Carbohydrate Polymers, 158*, 58–67.

Zhang, H., Nie, S., Guo, Q., Wang, Q., Cui, S. W., & Xie, M. (2018). Conformational properties of a bioactive polysaccharide from *Ganoderma atrum* by light scattering and molecular modeling. *Food Hydrocolloids, 84*, 16–25.

Zhang, M., Cui, S. W., Cheung, P. C. K., & Wang, Q. (2007). Antitumor polysaccharides from mushrooms: A review on their isolation process, structural characteristics and antitumor activity. *Trends in Food Science & Technology, 18*(1), 4–19.

Zhang, Y., Li, S., Wang, X., Zhang, L., & Cheung, P. C. K. (2011). Advances in lentinan: Isolation, structure, chain conformation and bioactivities. *Food Hydrocolloids, 25*(2), 196–206.

Zhang, H., Li, C., Ding, J., Lai, P. F. H., Xia, Y., & Ai, L. (2020). Structural features and emulsifying stability of a highly branched arabinogalactan from immature peach (*Prunus persica*) exudates. *Food Hydrocolloids, 104*, Article 105721.

Zhang, H., Zhao, T., Wang, J., Xia, Y., Song, Z., & Ai, L. (2020). An amendment to the fine structure of galactoxyloglucan from Tamarind (*Tamarindus indica* L.) seed. *International Journal of Biological Macromolecules, 149*, 1189–1197.

Zhao, T., Mao, G., Feng, W., Mao, R., Gu, X., Li, T., et al. (2014). Isolation, characterization and antioxidant activity of polysaccharide from *Schisandra sphenanthera*. *Carbohydrate Polymers, 105*, 26–33.